Re: 14594

Яндекс 360

19 июля 2025 г., 18:27
От кого: «RusAutoCon 2020» <rusautocon@gmail.com>
Кому: rvprikhodko@edu.hse.ru

Добрый день!

Отредактированная версия статьи получена. Благодарим вас за проведенную коррекцию.

Ваша статья с регистрационным номером 14594 прошла рецензирование и принята к публикации.
Оплатить оргвзнос Вы можете как от физического, так и от юридического лица.
От физического лица оргвзнос можно оплатить при помощи QR-кода по системе СБП или банковской картой (по ссылке с сайта конференции https://rusautocon.org/index.html).
Для оплаты оргвзноса от юридического лица бланк договора будет направлен по запросу на электронный адрес конференции.
Оплату необходимо произвести с условием, чтобы к нам деньги поступили не позже 8 сентября 2025 г.

Также напоминаем Вам о необходимости предоставления цветных скан-копий дополнительных документов (https://rusautocon.org/registration-rus.html):
1. Заключения о возможности открытого опубликования (экспертное заключение об отсутствии в статье сведений, составляющих государственную тайну).
Название статьи должно быть указано на английском языке. Вся печать организации должна быть четко читаема.

2. Заключения комиссии внутреннего экспортного контроля (экспортное заключение).
Название статьи должно быть указано на английском языке. Вся печать организации должна быть четко читаема.

3. Анкеты-согласия на обработку персональных данных от каждого автора статьи. Шаблон анкеты доступен для скачивания по адресу https://rusautocon.org/registration-rus.html

Передача авторских прав на статью издательству IEEE Xplore осуществляется онлайн, ссылка будет направлена вам ближе к конференции.

В конференции предусмотрено три формата участия:
1) традиционный очный формат;
2) дистанционно в формате видеоконференции;
3) дистанционно в формате краткого on-line сообщения и дальнейшего стендового представления работы.
Заочного участия в конференции не предусмотрено.

Просим Вас до 18 августа сообщить выбранный Вами формат участия и регистрационный номер Вашего доклада, и напоминаем, что для участия в дистанционном формате необходимо до 1 сентября выслать презентацию в адрес оргкомитета.

Шаблоны презентаций доступны для скачивания на сайте конференции https://rusautocon.org/index.html на главной странице в нижней части.
Рабочими языками конференции являются русский и английский. Вы можете подготовить презентацию и сделать доклад на любом из них.

Программа конференции и расписание времени работы секций будут опубликованы по адресу https://rusautocon.org/programme-rus.html

Обращаем внимание, Оргкомитет не высылает уведомлений о начале работы секции, авторам необходимо самостоятельно следить за расписанием работы секции на сайте конференции в разделе "Программа конференции" https://rusautocon.org/programme-rus.html.

С уважением,
Оргкомитет RusAutoCon-2025

пт, 4 июл. 2025 г. в 16:52, RusAutoCon 2020 <rusautocon@gmail.com>:

Добрый день!

Ваша статья с регистрационным номером 14594 проверена корректором. Необходимо внести следующие изменения:

1) Задать абзацы уравнений: первая строка: нет; интервал перед: 12 пт, после: 12 пт, междустрочный: множитель 0,9.
Номер каждого уравнения вынести за пределы математического редактора и выровнять по правому краю колонки.
Уравнение выровнять по центру колонки с использованием табуляции, как в шаблоне издательства. Шаблон прикреплен в приложении к данному письму.

2) Перед рисунком 1 добавить в текст ссылку на него.

3) Перед таблицами 2-8 разместить в тексте ссылки на них.

Отредактированную версию статьи просим отправить до 10 июля.

С уважением,
Оргкомитет RusAutoCon-2025

сб, 21 июн. 2025 г. в 21:18, RusAutoCon 2020 <rusautocon@gmail.com>:

Добрый день
Уважаемые авторы, ваша регистрационная форма 14594 и статья получены. Ваш доклад зарегистрирован и направлен на рецензирование. Просьба при дальнейшей переписке через электронный ящик конференции всегда указывать этот номер в теме письма.
С уважением,
Оргкомитет RusAutoCon-2025

✉rusauto

ПРОГРАММА КОНФЕРЕНЦИИ

Перечень принятых докладов
(по состоянию на 25 июля 2025 г.)

№	Фамилии авторов, название доклада
	Секция 1. Автоматизация технологических процессов
14541	*V. Trofimov* On Designing an Intelligent System for Sintering Process Diagnostics
14552	*M.R. Gofurjonov, L.Ya. Xuramov, Yu. Pisetskiy* Using a Combination of Otsu Segmentation, Cubic Spline, and Gaussian Filter in Ultrasonograp Processing for Gallbladder Stone Identification
14555	*A. Margun, R. Iureva, K. Zimenko* State Estimation for Partially Unknown Nonlinear Systems via Observer-ML Fusion
14585	*A. Zaytsev, N. Dmitriev, E. Konnikov* Integration of Event-Driven Modeling and Stochastic Optimization Within Control Frameworks Energy Systems
14587	*S. Sidorova, A. Kouptsov, G. Dyachkov* Automated System of Substrates Positioning and Processing in Vacuum
14610	*V. Zakharov* Automation of Proactive Monitoring Processes of Complex Agrobiotechnical Objects
14612	*E.M. Portnov, Aung Kyaw Myo, A.V. Potapov* Methods for Efficient Utilization of IEC 60870-5-101/104 Telecontrol Communication Protocol Telemechanics Systems
63015	*I. Baybikov, V. Kozlovskiy, A. Starikov* Algorithm of Operation of the Digital Controller of the High-Speed Response Servo Drive with Synchronous Motor
63018	*V. Khokhlov, N. Yarda* Increasing the Efficiency of Operating Modes of Power Installations and Structures of Pumped Power Plants
	Секция 2. Математическое моделирование технологических процессов и технических
14497	*Zhai Yiming, M.S. Selezneva, Zhu Hang* Automatic Parking Trajectory Optimization: A Hybrid Genetic Algorithm with Q Learning
14498	*Zhu Hang, M.S. Selezneva, Zhai Yiming* Trajectory Planning of Heterogeneous Multi-Agent System Based on Soft Actor-Critic Algorith
14506	*I. Magomedov, M. Matygov, F.K. Dzamikhova* Analysis of the Impact of Legged-Wheels Asymmetry on the Ability to Locomotion Using Infor Computational Engineering Tools
14521	*Yu. Diachenko, N. Morozov, G. Orlov* Self-Timed Circuit Synthesis and Its Verification
14522	*Yu. Stepchenkov, Yu. Diachenko, D. Stepchenkov* Self-Timed Circuit Initialization
14523	*T.R. Abdullin, A.G. Isavnin* Intelligent Data Analysis in District Heating Systems: Predictive Diagnostics Using Machine Le
14530	*M. Skoptsov, A. Zubatova, S. Mosin* Noise-Immune Detector of PUCCH Signal Diversity Reception Based on Cholesky Decomposi
14539	*N. Shevko, E. Priimak, N. Bikeeva* The Use of Software Tools in the Study of the Crime Rate Using the Non-Parametric Sign Crite
14547	*M. Sokolov, A. Khodkevich* Application of Conformal Mappings to Determine the Location of a Rail Break
14559	*S.V. Sokolov, I.V. Reshetnikova, V.I. Yuhnov* Solving the Problem of High-Precision Spatial Orientation of Mobile Objects Based on Satellite

	Measurements in the Pre-Launch Preparation Mode
14568	*M.Y. Romashikhin* Digital Filtering Algorithms for Signal Processing in NoCs
63003	*N. Boldyrikhin, I. Sosnovsky* Optimization of the Processes of Monitoring the Energy Parameters of Computer Systems

Секция 3. Теория управления

14526	*Jia Tian, Lifei Zhang, Lilian Zhang, Hao Chen* A Buffer Length Selection Method for Systems with Random Measurement Delays
14531	*A.V. Lapin, N.E. Zubov, E.Yu. Zybin* Analytical Synthesis of Modal Control by Output for Fourth-Order Systems with Two Inputs an Outputs at Equal Indices of Controllability and Observability
14550	*S.A. Zhigalova, E.A. Shelenok* Decentralized Combined Control System for a Multi-Connected and Multi-Mode Plant with De

Секция 4. Интеллектуальные системы

14510	*L.Ya. Xuramov, X. Bustanov, Y.A. Imamova* Advanced Signal Processing Models in Smart Home Systems
14533	*I.V. Ushenina, E.A. Danilov* Programmable Artificial Neuron Module for Feedforward Neural Networks
14544	*E.S. Abramova, A.A. Orlov* A Neuron Splitting Algorithm with Weight Conservation for Adaptive Neural Networks
14557	*M. Poryvai, D. Namiot* On Natural Image Augmentation to Increase Robustness of Machine Learning Models
14558	*A. Lazarev* Design of Adaptive Control Systems for IoT Devices on the Tuya Development Platform Using Reinforcement Learning
14564	*O. Bulygina, A. Sokolov, M. Vorotilova* Situation Management of Multi-Stage Chemical-Technological Processes Using Fuzzy Co-Evol Metaheuristics
14577	*K. Zhernova* Combined Method for Designing Efficient Visualization Models Using Machine Learning for F Selection
14578	*A.A. Kobachenko, M.V. Murashov* Development of a Soft Sensor for Petroleum Product Quality Based on Machine Learning
14590	*S. Sariyev, G. Negmatova, A. Sayidkulov* Preparation Datasets Based on Artificial Intelligence Models and Classification Algorithms
14592	*L. Suleiman, S. Vlasov, Nguen Khac Tung* Deep Regression Based Model Predictive Contnrol Approach For Cooperative/Adaptive Cruise Systems
14594	*R. Prikhodko, A. Moshkin, A. Romanov* Segmentation of Vertebral Arteries on the MR Images
63016	*O.Yu. Maryasin, A. Plohotnyuk* Building Energy Consumption Control Based on Multi-Agent Reinforcement Learning

Секция 5. Гибкие производственные системы

	В данной секции пока нет принятых статей

Секция 6. Промышленная робототехника и мехатроника

14508	*P. Bezmen* Convergence Rate Analysis of the "Extended Kalman Filter – Adaptive Digital Filter" Algorithn
14512	*Peng Sikun, Guo Yuanyuan, M.S. Selezneva* Stochastic Path Optimization Method based on Gaussian Process
14514	*S.F. Jatsun, E.V. Saveleva, A.S. Pechurin* Mobile Medical Robotic Platform for Solving Logistics Problems
63017	*Yu.P. Filyushov, S.V. Gorelov, V.Yu. Filyushov* Cost-Effective Control of a Salient Poles Synchronous Permanent Magnet Machine

Секция 7. Системы технического зрения

14516	*H.N. Zaynidinov, L.Ya. Xuramov, M. Sanayev* Application of Optimal Wavelet Transform Models in Gastroenterological Signal Processing
14517	*S.V. Sokolov, D.V. Marshakov, I.V. Reshetnikova* Parametric Identification Field of Velocities of the Optical Flow and Estimation of its Intensity i Vision Systems
14519	*M.V. Khachumov, M.V. Shustova* Target Object Recognition Based on Invariants and Fast Neural Networks

14525	*A. Bobokhonov, L.Ya. Xuramov, M. Ahtamqulov* Development of a Hybrid Model of Digital Filter and Bicubic Spline Methods in Medical Image Preprocessing
14551	*A. Bobokhonov, L. Xuramov, A. Rashidov* Evaluation of the Effectiveness of Interpolation Methods in the Process of Image Size Standardi

Секция 8. Информационная безопасность промышленных систем автоматизаци

14492	*K. Zhernova* Identification of Vulnerabilities in the Visualization of Statistical Metrics for Software Using Ne Networks
14493	*I. Kotenko, I. Parashchuk* Fuzzy Assessment of the Reliability Level of Identifying Malicious Activity Signs in the Infrast Industrial Smart City
14511	*N. Mokrinskii, P. Sharikov* Methodology for Determining the Available Volume for Embedding Digital Watermarks in Java
14527	*A.H. Tantserov, E.A. Danilov* Enhancing Dynamic Signature Identification Accuracy through Reference Model Synthesis
14606	*P. Sobolev, I. Kotenko* Detecting Attacks on Web Applications: Using the Convolutional Neural Network, Multilayer P and Random Forest Models

Секция 9. Диагностика и надежность систем автоматического управления

14528	*V. Gvozdev, O. Bezhaeva, A. Rakipova* Development of Algorithms to Support Management of Cyberphysical Devices Based on Meası
14535	*J.F. Kurbanov, E.G. Khujamkulov, M.Y. Xokimjonov* Intellectual Diagnostics of the Blocks Electrical Centralization System at the Station
14571	*I. Sokolov, D. Khilko, G. Orlov* Synthesis of a Self-Timed Pipeline by Converting the Description of a Synchronous Analog

Segmentation of vertebral arteries on the MR images

R. Prikhodko
HSE University
Moscow, Russia
rvprikhodko@edu.hse.ru

A. Moshkin
OSU named after I.S. Turgenev
Orel, Russia
as.moshkin@internet.ru

A. Romanov
HSE University
Moscow, Russia
a.romanov@hse.ru

Abstract—**The vertebral arteries are one of the most important sources of blood supply to the brain, therefore any pathological changes in them can be the reason behind serious diseases. Magnetic Resonance Imaging (MRI) allows diagnosticians to examine main arteries, which is exceptionally important for effective diagnosis. However, because of the small size of arteries relative to full MRI scan diagnosticians may not be able to spot significant anomalies due to subjective factors. This paper proposes the development of an intelligent system based on neural network for the segmentation of vertebral arteries in clinical MRI images. The system provides comparative analysis in form of reports, assisting diagnosticians in accurately examining relatively small regions of vertebral arteries in clinical MRI images. The proposed service has the potential to significantly improve identification of any vertebral arteries related pathologies, which result in improving diagnostic quality.**

Keywords—Vertebral arteries, MRI, Neural Networks, Segmentation, Software Application

I. INTRODUCTION

The vertebral arteries [1] are one of the most important components of the circulatory system since it is responsible for supplying blood to brainstem and cerebellum. Considering their essential role in cerebral blood flow, any pathology such as stenosis, occlusion, or dissection [2], may lead to serious neurological changes in cerebral circulatory system. Therefore, early detection and accurate diagnosis of these pathologies are crucial for effective treatment and better patient outcomes. Vertebral arteries diseases, such as atherosclerosis, vertebral artery dissection, and congenital anomalies, often manifest through symptoms like dizziness, discoordination, and visual disturbances. However, these symptoms can be nonspecific, making it difficult to diagnose such conditions based solely on clinical presentation. Magnetic Resonance Imaging (MRI) [3] plays a large role in visualizing vertebral arteries and identifying deviations. MRI provides images of high resolution, which allows diagnosticians to examine structure and blood flow in these arteries. Despite its advantages, small size of vertebral arteries relative to clinical MRI images makes analysis of arteries more difficult even for experienced radiologists.

Artificial intelligence (AI) [4] has been an extremely powerful tool in many different fields, including medicine, where it assists in tasks such as image analysis and predicting diagnosis. AI-based systems have the ability automate complex tasks, which improves the accuracy and efficiency of medical imaging analysis and reduces reliance dependence on human factors. Neural networks [5] have shown remarkable success in image processing tasks, including segmentation [6]. Segmentation includes dividing an image into regions. For example, one of these region may be identified as a specific anatomical structure. Separating vertebral arteries from surrounding tissues can assist in creating detailed analysis.

The task of vertebral arteries segmentation can be further enhanced by creating a method that automatically calculates key metrics, such as arterial diameter. Furthermore, logging these results into a database for future references can ease the diagnostic process. Automation of these steps can eliminate human error, making sure that evaluations are consistent. This approach not only improves diagnostic accuracy but also shortens analysis time, which enables better patient care.

In this work the intelligent system based on neural network for the segmentation of vertebral arteries in clinical MRI images is proposed. The system is designed to provide a comprehensive solution that combines accurate segmentation, automated calculation of metrics and data logging, improving the diagnostic process and assisting diagnosticians in making correct decisions.

II. RELATED WORK

A. Traditional Image Processing Techniques

Traditional methods of segmenting vascular structures relied heavily on math-based techniques, such as Gabor filters. These filters combine sinusoidal functions with Gaussian kernels and are effective in capturing local frequency and orientation information. For example, in [7] Gabor filters were used to improve the segmentation of vascular structures by analyzing texture patterns on MRI images. This approach enhanced the detection of vascular networks, making it suitable for completing tasks that require high precision. Similarly, [8] demonstrated the integration of Gabor filters into neural network architectures, leveraging their ability of extracting specific features and suppressing noise.

Another method is the Frangi filter, which was specifically designed for tubular structure segmentation. The Frangi filter analyzes the Hessian matrix [9] of an image to identify vessel-like structures based on eigenvalues, which separates tubular shapes from other.structures. In [10] the Frangi filter was used to preprocess MRI images, highlighting the vessels in order to distinguish vascular structures from surrounding tissues. This preprocessing step significantly improved the performance of segmentation tasks, specifically in complex datasets with a lot of noise and extremely low contrast.

B. Deep Learning Approaches

With the recent explosion in popularity of deep learning, convolutional neural networks (CNNs) have become the staple for medical image segmentation. The FC-ResNet architecture [11] has gained attention for its effectiveness in signature

verification tasks, particularly in multilingual settings. Built upon the ResNet18 backbone, FC-ResNet integrates residual connections to enable deeper network training without vanishing gradients. Additionally, the use of Convolutional Block Attention Modules (CBAM) enhances the model's ability to focus on both channel-wise and spatial features, allowing it to adaptively emphasize informative regions in signature images.

Recent studies have explored the integration of traditional filters with deep learning models to enhance segmentation accuracy. For example, [10] proposed a hybrid approach where the Frangi filter was used for pretraining a neural network on unlabeled data. This strategy reduced the dependency on large annotated datasets and improved the model's ability to generalize across different imaging conditions. Similarly, [8] Gabor filters combined with segmentation model to leverage texture-based features while benefiting from the learning capabilities of deep networks. These hybrid approaches demonstrate the potential of combining classical image processing techniques with modern machine learning methods.

Some neural network architectures were specifically designed for medical segmentation purposes. One of these models is HaTU-Net [12]. The author of architecture proposes an addition of harmonic attention layer.

The proposed model was then compared to others via ovaries segmentation. The results of comparison are demonstrated below in Table 1.

TABLE I.   Model comparison for ovary segmentation

Models	Accuracy [13]	Dice [14]	IoU [15]
U-Net [6]	96.89 ± 0.02	87.89 ± 0.08	77.54 ± 0.12
Attention U-Net [16]	96.41 ± 0.02	86.02 ± 0.09	74.89 ± 0.13
R2U-Net [17]	95.73 ± 0.03	83.31 ± 0.12	71.49 ± 0.15
U-Net++ [17]	97.14 ± 0.02	87.88 ± 0.10	77.72 ± 0.13
DeepLabv3+ [18]	96.99 ± 0.02	86.66 ± 0.11	76.21 ± 0.14
HaTU-Net [12]	97.55 ± 0.01	90.01 ± 0.07	80.72 ± 0.11

III. Methods

A. Dataset

The dataset used in this study consists of 97 MRI images in JPEG format. These images were provided by Andrey Moshkin from Orel State University named after I.S. Turgenev. Each image has a corresponding mask that highlights the vertebral arteries. The dataset consists primarily of two MRI images types: T1 and T2.

T1 images are service images that are done right before medical examination. These MRI images highlight liquor with a black color and vessels with a white color. However, the edges between different structures are blurry, which makes it significantly more difficult to perform any segmentation tasks. On the other hand, T2 images are more fitting when it comes to strictly highlighting arteries and vessels as shown in Figure 1, which was solidified even further after running multiple segmentation tests.
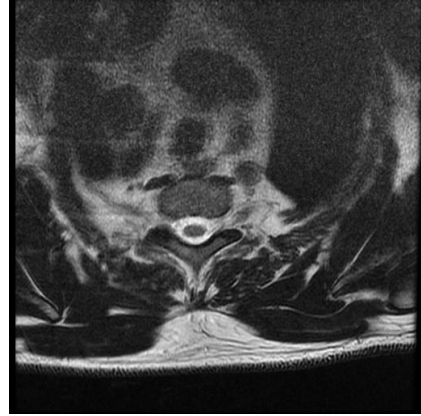

Fig. 1.   An example of T2 image

Due to abnormal differences between T1 and T2 images, it was decided to keep T2 images only, which leaves dataset with only 65 pairs of images and masks. Then the rest of the dataset was split into training and validation samples with the ratio of 55:10. Later on the dataset was extended using augmentations.

B. Preprocessing Methods

Noise in MRI images can significantly mess with segmentation performance. To address this, several denoising methods are applied during preprocessing separately.

Non-local means (NLM) filter [19] is a filter that works by replacing the intensity of each pixel with a weighted average of intensities from other pixels in the image. The weights are determined based on the similarity between local neighborhoods of pixels. The NLM filter is described using the following equation:

$$I(p) = \sum_{q \in \Omega} w(p, q) * I(q), \qquad (1)$$

where $I(q)$ is the value of q pixel, $w(p, q)$ is weight of similarity between p and q patches, and Ω is the area of search.

CurvatureFlow (CF) filter [20] is a type of filter based on the evolution of surface curvature that preserves important geometric features. An image is treated as a surface in three-dimensional space, where pixel intensity represents height. Filtering is carried out by deforming this surface in a way that is governed by the curvature of the intensity level. The surface "flows" in a direction that reduces its curvature.

Compared to the classical Gaussian filter, which blurs everything including edges, the CurvatureFlow filter smooths only noise while preserving significant structures such as object boundaries. The CurvatureFlow filter is described by the following equation:

$$\frac{\partial I}{\partial t} = |\nabla I| * k, \qquad (2)$$

where $I(x, y, t)$ is the image at time t, $|\nabla I|$ is the image gradient, and k is the curvature on the intensity level.

Frangi filter, which was specifically designed for tubular structure segmentation. It separates tubular shapes from other

structures by analyzing Hessian matrix in order to compute eigenvalues. Ultimately, Frangi filter aims to improve the visibility of vertebral arteries.

C. Segmentation Model and Loss Functions

The segmentation task is performed using the fully convolutional ResNet architecture [11]. The ResNet architecture was also slightly changed in order to increase segmentation accuracy:

- The model can only be trained using one-channel images (grayscale).

- Input and output layers were changed to work with 512x512 resolution images.

The model is then trained on the preprocessed dataset using a wide variety of loss functions to ensure the best performing combination of machine learning methods suited for this task is found.

After combining every single preprocessing technique and loss function, each instance is trained using Adam optimizer [21] with a learning rate of 1×10^{-3} for 200 epochs. Each instance is then evaluated using precision [22], recall [22], Dice and IoU and the best performing model is chosen.

D. Vertebral Arteries Metrics Calculation

Following segmentation, the size of the vertebral arteries is calculated using a known pixel-wise scale to find the diameter, area, and other relevant metrics of the arteries. These measurements are crucial for diagnosing vertebral arteries pathologies.

E. Database and Software

In order to store the parameters of vertebral arteries and facilitate tracking and analysis of metrics, a dedicated database is developed. This database stores segmented images, calculated metrics, and patient information. With the help of database, clinicians will be able to monitor changes in the dimensions of arteries over time.

Additionally, a software application is created to provide a user-friendly interface for the entire system. The application allows diagnosticians to upload MRI images, view the results of segmentation, patient information and automatically calculated vertebral arteries data. The application will automatically perform image preprocessing, metrics calculation, database logging and report generation, streamlining the diagnostic process.

IV. ACHIEVED RESULTS USING SEGMENTATION MODEL

Judging by results highlighted in the Tables 2 through 5 the best instance is the combination of CurvatureFlow filter and Dice + BCE loss function.

However, this result can only be considered unsatisfactory at best. In order for segmentation model to be practically useful, the Dice metric should at least be 70%. The best performing model only reaches 9.3%, which is far below optimal. The CF + DiceBCE model still makes a lot of errors with vertebral artery segmentation.

TABLE II. RESULTS OF SEGMENTATION ON A NON-PREPROCESSED DATA

Loss Functions	Metrics			
	Recall	Precision	Dice	IoU
MSE [23]	0.996	0.008	0.017	0.008
BCE with Logits [24]	0.004	0.861	0.008	0.004
Dice [14]	0.994	0.008	0.017	0.008
Dice + BCE [25]	0.051	0.363	0.089	0.047
IoU [15]	0.035	0.298	0.068	0.035
Focal [26]	0.994	0.008	0.017	0.008
Tversky [27]	0.037	0.307	0.067	0.035
Focal + Tversky [28]	0.000	1.000	0.001	0.000
LovaszHinge [29]	0.000	1.000	0.001	0.000
ComboLoss [30]	0.000	1.000	0.001	0.000

TABLE III. RESULTS OF SEGMENTATION ON A CF-FILTERED DATA

Loss Functions	Metrics			
	Recall	Precision	Dice	IoU
MSE [23]	0.996	0.008	0.017	0.008
BCE with Logits [24]	0.002	0.963	0.005	0.002
Dice [14]	0.994	0.008	0.017	0.008
Dice + BCE [25]*	**0.053**	**0.376**	**0.093**	**0.049**
IoU [15]	0.04	0.309	0.072	0.037
Focal [26]	0.003	0.955	0.007	0.003
Tversky [27]	0.034	0.334	0.062	0.032
Focal + Tversky [28]	0.032	0.279	0.059	0.003
LovaszHinge [29]	0.000	1.000	0.001	0.000
ComboLoss [30]	0.958	0.008	0.016	0.008

* marks the best overall result

TABLE IV. RESULTS OF SEGMENTATION ON A NLM-FILTERED DATA

Loss Functions	Metrics			
	Recall	Precision	Dice	IoU
MSE [23]	1.000	0.008	0.017	0.008
BCE with Logits [24]	0.000	1.000	0.001	0.000
Dice [14]	0.996	0.008	0.017	0.008
Dice + BCE [25]	0.037	0.397	0.075	0.039
IoU [15]	0.001	0.825	0.067	0.035
Focal [26]	0.031	0.362	0.003	0.001
Tversky [27]	0.039	0.377	0.057	0.029
Focal + Tversky [28]	0.000	1.000	0.072	0.038
LovaszHinge [29]	0.000	1.000	0.001	0.000
ComboLoss [30]	0.000	1.000	0.001	0.000

TABLE V. RESULTS OF SEGMENTATION ON A FRANGI-FILTERED DATA

Loss Functions	Metrics			
	Recall	Precision	Dice	IoU
MSE [23]	0.986	0.008	0.017	0.008
BCE with Logits [24]	0.000	1.000	0.001	0.000
Dice [14]	0.999	0.008	0.017	0.008
Dice + BCE [25]	0.027	0.299	0.050	0.025
IoU [15]	0.011	0.290	0.022	0.011
Focal [26]	0.000	1.000	0.001	0.000
Tversky [27]	0.013	0.151	0.025	0.012
Focal + Tversky [28]	0.002	0.242	0.038	0.019
LovaszHinge [29]	0.000	1.000	0.001	0.000

Loss Functions	Metrics			
	Recall	Precision	Dice	IoU
ComboLoss [30]	0.973	0.008	0.016	0.008

Such inferior performance can be explained by an unoptimized dataset. There are simply not enough images in the dataset in order to train the segmentation model effectively. The data varies significantly in terms of scale and perspective. No additional mapped images are available online to expand the dataset. It should be noted that the problem of small datasets is common [31], and we need to find approaches to overcome this problem and still achieve acceptable quality of the model. The next section is devoted to this.

V. ALTERNATIVE METHODS

The initial idea for implementing the neural network module of the intelligent system for vertebral artery segmentation was as follows:

- Perform segmentation of the vertebral arteries on MRI images.

- Convert the segmentation results into vertebral artery dimensions.

After analyzing the performance of the segmentation model, an alternative approach to solving the segmentation problem was developed, based on the fact that vertebral arteries appear as circular shapes on MRI images:

- Predict the size of the vertebral arteries.

- Predict positions of the vertebral arteries.

- Draw a circle with predicted radius with the centers located in predicted positions.

The two found diameters were stored in a tuple. Furthermore, combining the images and a diameters tuple allowed to create an entirely separate dataset.

For predicting the sizes, the ResNet50 model was chosen for training. The classifier architecture was modified so that the model would predict the diameters of the two vertebral arteries:

- A fully connected layer with an input size matching the image resolution and an output of 2048, with Dropout set to 0.3;

- A fully connected layer with an input of 2048, an output of 256, and Dropout set to 0.2;

- A final linear layer with an input of 256 and an output of 2 (representing the diameters of the vertebral arteries).

The model was then trained using the Mean Squared Error (MSE) loss function. Adam optimizer was used with a learning rate of 1×10^{-4}. A learning rate scheduler was also employed, which reduces the learning rate when the validation metric plateaus.

After training, the results were evaluated using the MAE and RMSE metrics. Additionally, the relative error and coefficient of variation were calculated. These metrics are commonly used in medical tools for assessing the dimensions of vascular structures.

To determine the positions, a method similar to the artery diameter estimation approach was applied:

- A function was implemented to convert a mask into coordinates of the form (x, y), where x and y are pixel values in the range from 0 to 512 (image resolution).

- A regression model was trained to predict these coordinates.

The position detection function was implemented using the measure method from the scikit-image library. The ResNet101 architecture was selected for training, with the classifier modified as follows:

- A fully connected layer with input size matching the image resolution and an output of 1024, with Dropout set to 0.25;

- A fully connected layer with input of 1024, output of 256, and Dropout set to 0.2;

- A final linear layer with input of 256 and output of 4 (representing the pixel coordinates of the vertebral arteries).

To evaluate the results, a function was implemented to calculate the Euclidean distance:

$$d(p, q) = \sqrt{\sum_{i=1}^{n} (p_i - q_i)^2}, \qquad (3)$$

where $p = (p_1, p_2, ..., p_n)$ are the true coordinates of the artery center, and $q = (q_1, q_2, ..., q_n)$ are the predicted coordinates.

The model was trained using the MSE loss function, the Adam optimizer with a learning rate of 1×10^{-4}, and the previously mentioned learning rate scheduler.

VI. TWO-STEP SEGMENTATION RESULTS

NLM-based and Frangi-based are the best performing models according to Tables 6 and 7 when it comes to predicting diameters. However, it was decided to continue working with an NLM-based model since it has lower relative error and coefficient of variance, which is crucial for consistent predictions.

TABLE VI. RESULTS OF SIZE PREDICTION (BOTH ARTERIES)

Filters	Metrics			
	MAE (pixels)	RMSE (pixels)	Relative Error (%)	CV (%)
No filters	1.22	1.52	20.25	13.46
CF	1.19	1.46	19.80	9.19
NLM*	**1.06**	**1.30**	**14.95**	**4.05**
Frangi	1.00	1.39	16.94	5.26

TABLE VII.   Results of position prediction

Artery	Euclidean distance (pixels)			
	No filters	CF	NLM*	Frangi
Left	11.57	11.56	**11.01**	12.35
Right	13.08	12.41	**12.79**	12.41
Both	12.32	11.99	**11.90**	12.38

For positions predicting the NLM-based model was chosen since it produces the lowest Euclidean distance. However, it is worth mentioning that position predictions are far from optimal due to dataset being too small. Source code for models training can be found on GitHub [32].

To combine the results of the two separate neural networks, a black image with a masks matching resolution (512x512) was created. Then, two white circular objects were drawn using the diameters predicted by the first model at the positions determined by the second model. The evaluation results of the step-by-step segmentation are presented in the Table 8.

TABLE VIII.   Diameter + position evaluation

Model	Metrics			
	Recall	Precision	Dice	IoU
Diameter + position	0.031	0.025	0.025	0.014
Diameter + initial position	**0.611**	**0.964**	**0.742**	**0.595**

For further development, it was decided to use the step-by-step segmentation model due to its stable performance. The classic segmentation model fails to accomplish the task because it cannot reliably detect the shape of the vertebral arteries.

To address the issue of position detection during application development, it is necessary to provide the user with a convenient way to adjust the positions of the arteries.

VII.   Software application

To facilitate working with the trained models, an application was also developed. It allows users to upload anonymized patient data and MRI images for further analysis. Since the models predict measurements in pixels, the user is required to input the FOV value to convert the sizes from pixels to millimeters.

After analyzing the images with the models, the user can manually adjust the predicted diameters and positions of the vertebral arteries. The analysis results can also be saved to a database and reloaded later.

In the artery position viewing window, users are provided with the ability to review and edit the positions of the vertebral arteries. The window interface includes:

- The MRI image overlaid with circles which diameters correspond to the predicted or manually adjusted values;

- A ComboBox for artery selection, enabling the user to choose which artery to adjust. Once selected, a MouseDrag event is triggered, allowing the user to correct the predicted positions using the mouse cursor;

- A slider to adjust the transparency of the circles (from 10% to 100%);

To ensure correct saving and the ability to revert to the predicted values, the database must include fields for both the predicted and modified values. Application source code can be found on a separate GitHub [33].

VIII.   Conclusion

The proposed methodology addresses several key challenges in vertebral artery segmentation, including the small size of the arteries relative to the full MRI image and the need for precise measurements of arterial dimensions. By combining sets of preprocessing techniques, segmentation model, and a comprehensive database for storing results, the system provides a powerful tool for clinicians to diagnose and monitor any vertebral arteries pathologies.

Using the fact that vertebral arteries are presented with circular shape the manual segmentation model was developed. With the use of initial positions the segmentation model performs with the $Dice = 0.742$.

References

[1]   S. Standring, "Gray's anatomy international edition: The anatomical basis of clinical practice," 2020.

[2]   L. R. Caplan and J. Van Gijn, "Clinical manifestations," *Stroke Syndr. Third Ed.*, pp. 1–328, Jan. 2012, doi: 10.1017/CBO9781139093286.

[3]   C. Westbrook and J. Talbot, "MRI in practice," p. 395, 2019.

[4]   H. J. Ian Goodfellow, Yoshua Bengio, Aaron Courville, "Deep learning," *Genet. Program. Evolvable Mach.*, vol. 19, no. 1–2, pp. 305–307, 2018.

[5]   M. Islam, G. Chen, and S. Jin, "An Overview of Neural Network," *Am. J. Neural Networks Appl.*, vol. 5, no. 1, p. 7, 2019, doi: 10.11648/J.AJNNA.20190501.12.

[6]   W. Weng and X. Zhu, "U-Net: Convolutional Networks for Biomedical Image Segmentation," *IEEE Access*, vol. 9, pp. 16591–16603, May 2015, doi: 10.1109/ACCESS.2021.3053408.

[7]   R. Mehrotra, K. R. Namuduri, and N. Ranganathan, "Gabor filter-based edge detection," *Pattern Recognit.*, vol. 25, no. 12, pp. 1479–1494, 1992, doi: 10.1016/0031-3203(92)90121-X.

[8]   D. Alblas, C. Brune, and J. M. Wolterink, "Deep Learning-Based Carotid Artery Vessel Wall Segmentation in Black-Blood MRI Using Anatomical Priors," p. 24, Dec. 2021, doi: 10.1117/12.2611112.

[9]   W. C. Thacker, "The role of the Hessian matrix in fitting models to measurements," *J. Geophys. Res. Ocean.*, vol. 94, no. C5, pp. 6177–6196, May 1989, doi: 10.1029/JC094IC05P06177.

[10] G. Shi, H. Lu, H. Hui, and J. Tian, "Benefit from public unlabeled data: A Frangi filtering-based pretraining network for 3D cerebrovascular segmentation," *Med. Image Anal.*, Dec. 2023, doi: 10.1016/j.media.2024.103442.

[11] P. Ghosal, L. Nandanwar, S. Kanchan, A. Bhadra, J. Chakraborty, and D. Nandi, "Brain tumor classification using ResNet-101 based squeeze and excitation deep neural network," *2019 2nd Int. Conf. Adv. Comput. Commun. Paradig. ICACCP 2019*, Feb. 2019, doi: 10.1109/ICACCP.2019.8882973.

[12] V. K. Singh *et al.*, "HaTU-Net: Harmonic Attention Network for Automated Ovarian Ultrasound Quantification in Assisted Pregnancy," *Diagnostics 2022, Vol. 12, Page 3213*, vol. 12, no. 12, p. 3213, Dec. 2022, doi: 10.3390/DIAGNOSTICS12123213.

[13] B. Liu and M. Udell, "Impact of Accuracy on Model Interpretations," Nov. 2020. https://doi.org/10.48550/arXiv.2011.09903

[14] D. Bell and C. Moore, "Dice similarity coefficient," *Radiopaedia.org*, Mar. 2020, doi: 10.53347/RID-75056.

[15] D. Zhou *et al.*, "IoU Loss for 2D/3D Object Detection," *Proc. - 2019 Int. Conf. 3D Vision, 3DV 2019*, pp. 85–94, Aug. 2019, doi: 10.1109/3DV.2019.00019.

[16] O. Oktay et al., "Attention U-Net: Learning Where to Look for the Pancreas," Apr. 2018. https://doi.org/10.48550/arXiv.1804.03999

[17] K. Dutta, "Densely Connected Recurrent Residual (Dense R2UNet) Convolutional Neural Network for Segmentation of Lung CT Images," Feb. 2021. https://doi.org/10.48550/arXiv.2102.00663

[18] L. C. Chen, Y. Zhu, G. Papandreou, F. Schroff, and H. Adam, "Encoder-Decoder with Atrous Separable Convolution for Semantic Image Segmentation," *Lect. Notes Comput. Sci.*, vol. 11211 LNCS, pp. 833–851, Feb. 2018, doi: 10.1007/978-3-030-01234-2_49.

[19] B. Liu and J. Liu, "Overview of image noise reduction based on non-local mean algorithm," *MATEC Web Conf.*, vol. 232, Nov. 2018, doi: 10.1051/MATECCONF/201823203029.

[20] A. El, A. Elmoataz, and A. Sadi, "On the mean curvature flow on graphs with applications in image and manifold processing," *Proc. IEEE Int. Conf. Comput. Vis.*, pp. 697–704, 2013, doi: 10.1109/ICCV.2013.92.

[21] D. P. Kingma and J. L. Ba, "Adam: A Method for Stochastic Optimization," 3rd Int. Conf. Learn. Represent. ICLR 2015 - Conf. Track Proc., Dec. 2014. https://doi.org/10.48550/arXiv.1412.6980

[22] D. M. W. Powers and Ailab, "Evaluation: from precision, recall and F-measure to ROC, informedness, markedness and correlation," Oct. 2020. https://doi.org/10.48550/arXiv.2010.16061

[23] S. Kato and K. Hotta, "MSE Loss with Outlying Label for Imbalanced Classification". Jul. 2021. https://doi.org/10.48550/arXiv.2107.02393

[24] T. Kobayashi, "Two-Way Multi-Label Loss," *Proc. IEEE Comput. Soc. Conf. Comput. Vis. Pattern Recognit.*, vol. 2023-June, pp. 7476–7485, 2023, doi: 10.1109/CVPR52729.2023.00722.

[25] J. Su *et al.*, "DV-Net: Accurate liver vessel segmentation via dense connection model with D-BCE loss function," *Knowledge-Based Syst.*, vol. 232, p. 107471, Nov. 2021, doi: 10.1016/J.KNOSYS.2021.107471.

[26] T. Y. Lin, P. Goyal, R. Girshick, K. He, and P. Dollar, "Focal Loss for Dense Object Detection," *IEEE Trans. Pattern Anal. Mach. Intell.*, vol. 42, no. 2, pp. 318–327, Feb. 2020, doi: 10.1109/TPAMI.2018.2858826.

[27] S. S. M. Salehi, D. Erdogmus, and A. Gholipour, "Tversky loss function for image segmentation using 3D fully convolutional deep networks," *Lect. Notes Comput. Sci.*, vol. 10541 LNCS, pp. 379–387, Jun. 2017, doi: 10.1007/978-3-319-67389-9_44.

[28] N. Abraham and N. M. Khan, "A novel focal tversky loss function with improved attention u-net for lesion segmentation," *Proc. - Int. Symp. Biomed. Imaging*, vol. 2019-April, pp. 683–687, Apr. 2019, doi: 10.1109/ISBI.2019.8759329.

[29] M. Berman, A. R. Triki, and M. B. Blaschko, "The Lov\'asz-Softmax loss: A tractable surrogate for the optimization of the intersection-over-union measure in neural networks," *Proc. IEEE Comput. Soc. Conf. Comput. Vis. Pattern Recognit.*, pp. 4413–4421, May 2017, doi: 10.1109/CVPR.2018.00464.

[30] S. A. Taghanaki *et al.*, "Combo loss: Handling input and output imbalance in multi-organ segmentation," *Comput. Med. Imaging Graph.*, vol. 75, pp. 24–33, Jul. 2019, doi: 10.1016/J.COMPMEDIMAG.2019.04.005.

[31] D. A. Lyutkin, *et al.*, "Segmenting Prostate Cancer on TRUS Images with a Small Dataset: A Comprehensive Methodology," *2023 International Russian Smart Industry Conference (SmartIndustryCon)*, pp. 454-459, 2023, doi: 10.1109/SmartIndustryCon57312.2023.10110773.

[32] rvprikhodko/ VA_model_train: Model training source code. URL: https://github.com/rvprikhodko/VA_model_train

[33] rvprikhodko/SA_VA: Application source code. URL: https://github.com/rvprikhodko/SA_VA